Atmospheric Environment 180 (2018) 69–78

Contents lists available at ScienceDirect

Atmospheric Environment

journal homepage: www.elsevier.com/locate/atmosenv

Assessing the impacts of seasonal and vertical atmospheric conditions on air quality over the Pearl River Delta region

Cheuk Hei Marcus Tong[a], Steve Hung Lam Yim[a,b,*], Daniel Rothenberg[c], Chien Wang[c], Chuan-Yao Lin[d], Yongqin David Chen[a,b], Ngar Cheung Lau[a,b]

[a] Department of Geography and Resource Management, The Chinese University of Hong Kong, Hong Kong, China
[b] The Institute of Environment, Energy and Sustainability, The Chinese University of Hong Kong, Hong Kong, China
[c] Center for Global Change Science, Massachusetts Institute of Technology, Cambridge, MA, USA
[d] Research Center for Environmental Changes, Academia Sinica, Taipei, Taiwan

ARTICLE INFO

Keywords:
Air quality
Climate change
Trans-boundary air pollution
Principal component regression
Generalized linear models

ABSTRACT

Air pollution is an increasingly concerning problem in many metropolitan areas due to its adverse public health and environmental impacts. Vertical atmospheric conditions have strong effects on vertical mixing of air pollutants, which directly affects surface air quality. The characteristics and magnitude of how vertical atmospheric conditions affect surface air quality, which are critical to future air quality projections, have not yet been fully understood. This study aims to enhance understanding of the annual and seasonal sensitivities of air pollution to both surface and vertical atmospheric conditions. Based on both surface and vertical meteorological characteristics provided by 1994–2003 monthly dynamic downscaling data from the Weather and Research Forecast Model, we develop generalized linear models (GLMs) to study the relationships between surface air pollutants (ozone, respirable suspended particulates, and sulfur dioxide) and atmospheric conditions in the Pearl River Delta (PRD) region. Applying Principal Component Regression (PCR) to address multi-collinearity, we study the contributions of various meteorological variables to pollutants' concentration levels based on the loading and model coefficient of major principal components. Our results show that relatively high pollutant concentration occurs under relatively low mid-level troposphere temperature gradients, low relative humidity, weak southerly wind (or strong northerly wind) and weak westerly wind (or strong easterly wind). Moreover, the correlations vary among pollutant species, seasons, and meteorological variables at various altitudes. In general, pollutant sensitivity to meteorological variables is found to be greater in winter than in other seasons, and the sensitivity of ozone to meteorology differs from that of the other two pollutants. Applying our GLMs to anomalous air pollution episodes, we find that meteorological variables up to mid troposphere (~700 mb) play an important role in influencing surface air quality, pinpointing the significant and unique associations between meteorological variables at higher altitudes and surface air quality.

1. Introduction

Air pollution is strongly influenced by meteorological conditions. For example, previous studies have reported that heat waves and droughts have a significant contribution on ozone (O_3) and particular matter and air-quality-related mortality (Fischer et al., 2004; Filleul et al., 2006). There is a rising concern that as a result of climate change, air quality in cities will degrade in the future (IPCC, 2014), but the mechanisms driving these changes have yet to be fully understood. Previous work has studied the relationship between air pollution and various meteorological conditions, but findings vary among different studies. For instance, the formation and removal of surface O_3 are enhanced by increases in temperature and ultraviolet radiation. Previous studies have adopted air quality models to examine the influence of meteorological conditions on increases in O_3 concentration (Sillman and Samson, 1995; Sillman, 1999). The magnitude of this influence is however still uncertain (Cuchiara et al., 2014). On the other hand, concentration of respirable suspended particulates (RSP) was revealed to be strongly correlated with low relative rainfall and humidity (Chan and Kwok, 2001), while other studies found that RSP concentration is associated with wind direction (Chan and Kwok, 2001; Cheng and Lam, 1998; Peng et al., 2011). Some studies have combined theoretical interactions between meteorology and air pollutants to investigate the overall correlation, but the occurrence and magnitude of these

* Corresponding author. Department of Geography and Resource Management, The Chinese University of Hong Kong, Hong Kong, China.
E-mail address: steveyim@cuhk.edu.hk (S.H.L. Yim).

https://doi.org/10.1016/j.atmosenv.2018.02.039
Received 30 August 2017; Received in revised form 6 February 2018; Accepted 19 February 2018
Available online 23 February 2018
1352-2310/

interactions have yet to be well understood (e.g., Samet et al., 1998).

Correlations between meteorological and air quality variables can vary from region to region because of differential meteorological patterns in terms of synoptic, mesoscale, and turbulent scales (Pielke and Uliasz, 1998), as well as changing spatial patterns of pollutant emissions (Fiore et al., 2012). IPCC (2014) reported that there are insufficient studies focusing on the Asia and Pacific regions, where regional monsoons dominate seasonal climate variability. The Pearl River Delta (PRD) region, which accommodates tens of millions of inhabitants in major urban areas, has suffered from complex regional air pollution problems due to escalating anthropogenic emissions and its unique geography and climatology settings (Wang et al., 2003; Wu et al., 2005; Zhang et al., 2015). Several studies have highlighted a relationship between atmospheric conditions and air quality over the region (Cheng and Lam, 1998; Zhao et al., 2016). Given that the climate is projected to change, to investigate how climate change impacts on air quality requires a systematic and clear understanding of the current meteorology-air quality relationship.

While statistical approaches were commonly applied to understand influences of meteorology on air quality, majority of them focused on the sensitivity of air quality to surface meteorological conditions (Li et al., 2014; Luo et al., 2017; Ramsey et al., 2014; Tai et al., 2012; Zhang et al., 2015). Only few of them have explored the sensitivity of air quality to vertical atmospheric profiles i.e. temperature and wind profiles and developed regression models based on both surface and vertical meteorological characteristics, and comprehensively described influences of surface and upper level meteorology on various pollutants in different seasons. Atmospheric stability, normally quantified by meteorological characteristics among different altitudes, has a significant influence on re-circulating polluted air within the PRD and it mixes pollutants emitted from varying sources (Lo et al., 2006), as well as allows pollutants to accumulate and chemically react under stagnant airflow conditions (Wu et al., 2005). The Bulk Richardson Number, an atmospheric stability metric, has been shown to be associated with surface stability (Zoumakis and Kelessis, 1991), and has been applied to examine its effect on air quality through vertical mixing (Jeričević and Grisogono, 2006). However, none of them have applied separately the component of these metrics, which are the meteorological variables at different altitudes, to investigate how meteorology influences the vertical transport of air pollutants and thus impacts air quality.

Furthermore, literature commonly focused on the effects of meteorology on O_3 and particulate matters, or indices that are used to represent air quality. A comprehensive analysis of influences of meteorology on various pollutants has yet to be available. For example, while sulfur dioxide – an important particulate matter precursor – is strongly influenced by atmospheric characteristics (Cheng and Lam, 1998; Meng et al., 2010). How meteorology at different attitudes affects sulfur dioxide has yet to be fully understand. A multi-pollutant analysis is necessary to provide vulnerable information for policy makers and atmospheric scientists.

The aim of this study is to develop linear models using dynamic downscaling meteorological data along with air quality observations, and to evaluate the sensitivity of each air pollutant to surface and upper level meteorological variables. This allows us to understand the sensitivities of O_3, RSP and SO_2 concentration to both surface and vertical atmospheric conditions in the densely populated PRD region, and particularly to explain recently observed extreme anomalies of air quality in the PRD region.

2. Data and methods

2.1. Site selection

The PRD region is selected in this study due to two primary reasons: it has a large population living under rising concerns about air pollution, and it has a complicated air quality–meteorology relationship due to unique geographical and climatic conditions. The PRD region is a large low-lying area surrounded by the hilly coast of southern China. The region is often regarded as an emerging megacity and is considered a fast-growing economic area (Wang et al., 2014). It features nine major cities and two special administrative regions (SARs), Hong Kong and Macao. The climate of PRD is influenced by the Asian monsoon, with prevailing winds from the northeast in winter, from the east in spring and autumn, and from the southwest in summer (Wang et al., 2001). Most rainstorms occur during the warm period of April to September. Air pollution in the PRD is typically attributed to emission sources at alternating spatial scales (local, regional in PRD and beyond the PRD region) under certain synoptic conditions (Huang et al., 2005; Luo et al., 2017; Wang et al., 2009). Local pollution is caused by intensive air pollutant emissions from different sources such as power plant, industry and mobile sources (Zheng et al., 2009). Additionally, monsoons sometimes transport pollutants along the coastline from adjacent areas into the PRD region.

Air pollution in the PRD region has a significant *trans*-boundary nature (Gu and Yim, 2016; Lee and Savtchenko, 2006). This study includes three air quality monitoring stations in Hong Kong due to their air quality characteristics and a better representation of regional air quality (see Fig. 1). The monitoring stations include Yuen Long (22.4440 °N, 114.0224 °E), Tung Chung (22.2886 °N, 113.9431 °E) and Tap Mun (22.4714 °N, 114.3608 °E). These stations represent different land-use types and have different surrounding geographic landscapes. Yuen Long station is located in a new town at the northwest of Hong Kong, with immediate exposure to *trans*-boundary air pollution. The sampling height of Yuen Long station is 25.0 m above ground. Tung Chung station is situated within a residential area in a new town on the north-western coast of Lantau Island. Tung Chung is surrounded by mountains on three sides (west, south and east), including Lantau Peak (934.0 m, second highest peak in Hong Kong) and Sunset Peak (869.0 m, third highest peak in Hong Kong). The sampling height of Tung Chung station is 27.5 m above ground. Tap Mun is a rural station located on Grass Island in north-eastern part of Hong Kong. The highest point of Grass Island is 125.0 m above sea level and the sampling height of Tap Mun station is 11.0 m above ground.

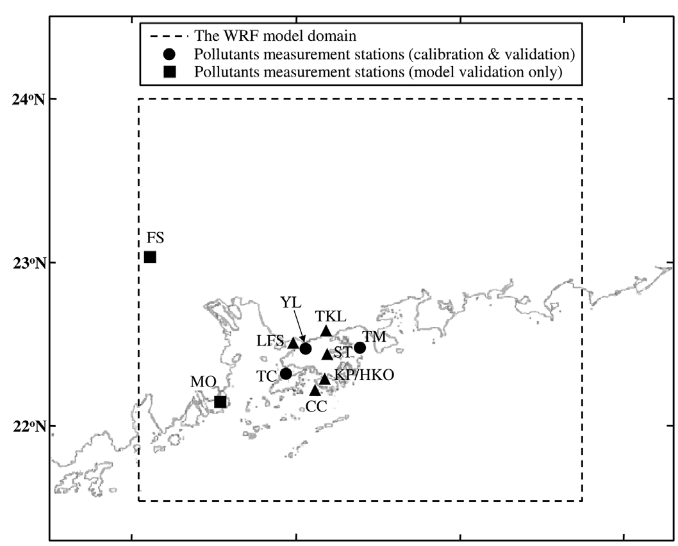

Fig. 1. The WRF model domains. The circle labels show the locations of air pollution measurements [Yuen Long (YL), Tung Chung (TC) and Tap Mun (TM)] for model calibration and validation. The square labels show the location of air pollution measurements [Foshan (FS) and Macau (MO)] outside Hong Kong used for model validation only. The triangular labels show the locations of weather stations [Lau Fau Shan (LFS), Shatin (SHA), Ta Kwu Ling (TKL), Cheung Chau (CC) and Kings Park/Hong Kong Observatory Headquarter (KP/HKO)] for our WRF validation.

Table 1
Meteorological variables used in the study.

Temperature (°C)	Temperature difference (°C)	Temperature – dew point difference (°C)	U wind component (m/s)	V wind component (m/s)
2m	2m–925 mb 925 mb–850 mb 850 mb–700 mb	2m 925 mb 850 mb 700 mb	10m 925 mb 850 mb 700 mb	10m 925 mb 850 mb 700 mb

2.2. Meteorological data

Several classical atmospheric stability indices are commonly used to explain various atmospheric interactions. For instance, meteorological studies often utilize stability indices to determine the possibility of thunderstorms. Such indices typically include the K-index (George, 1960) or Total-total index (Miller, 1972) and involve a combination of vertical temperature gradients, dew point-temperature differences and dew points measured at various altitudes (Bhattacharjee et al., 2007; Zhang et al., 2014). Other atmospheric stability indices, such as the Bulk Richardson Number, which uses virtual temperature differences, virtual temperature, and U and V wind components, have also been applied in air quality studies (Baklanov et al., 2002; Borger et al., 2008; Shir and Shieh, 1974).

The meteorological variables chosen in this study are referenced from the classical atmospheric stability indices. These include temperature, vertical temperature difference, humidity, U and V wind components, taken at four altitudes: surface level at 2m or 10m, 925 mb, 850 mb, 700 mb. The highest altitude (700 mb) is approximately 3000 m above the surface and also above where most anthropogenic aerosols are typically found (Table 1). Note that positive values of U and V wind components respectively indicate westerly and southerly winds.

We analyse meteorological variables representing atmospheric stability for the present year produced by simulations using the Weather Research and Forecasting Model (WRF) (Skamarock and Klemp, 2008). The WRF model – a commonly used non-hydrostatic mesoscale model – solves a set of atmospheric governing equations for weather prediction and climate projection. Our WRF model applies a dynamic downscaling approach to resolve the meteorology with two nesting domains (15 km and 5 km) and 45 uneven vertical levels. More details of the WRF model simulations are provided by Lin et al. (2015). To study recent variability in these variables we use the NCEP/NCAR reanalysis (NNR) data set (Kalnay et al., 1996; Kistler et al., 2001) over the recent past period (1994–2003) and then dynamically downscale to a spatial resolution of 5 km over east China. Bilinear interpolation is then applied to all the above grid data to derive point estimates of meteorological data at the three study sites.

2.3. Air quality data

This study focuses on three air pollutants: O_3, RSP and SO_2. These pollutants are selected based on three main reasons. First, these pollutants can represent the *trans*-boundary air pollution nature in the PRD region. They are all major air pollutants in the PRD and its neighbourhood areas, and produced from both local and non-local emission sources (Che et al., 2011; Wang and Lu, 2006). These pollutants can be potentially transported over long distances (Fiore et al., 2009). Their spatial footprint can thus be significantly influenced by variability in atmospheric stability and mixing. Second, they are often considered as indicator species for ambient air quality assessment and management in the PRD region due to their adverse influences on human health and vegetation (e.g. Wong et al., 2013). Third, their data availability can provide sufficient data for our analyses.

2.4. Statistical models

The sixteen meteorological variables used in this study are strongly correlated with one another, and we thus consider them to be collinear; up to thirteen variables have their Variance inflation factor (VIF) above a threshold of 10 which indicates significant multi-collinearity (Kutner et al., 2004), as shown in Fig. S1. Severe multi-collinearity can yield misleading results when analysing the statistical significance of correlations among time series of presumably-related fields.

We apply Principal Component Regression (PCR) to address this multicollinearity problem. PCR is a simple and non-parametric method to compress information in high-dimensional data sets, and has been used widely in geophysical studies, including ones related to air quality and meteorology (e.g., Abdul-Wahab et al., 2005; Hassanzadeh et al., 2008; Maenhaut et al., 1989; Rajab et al., 2013; Statheropoulos et al., 1998; Tai et al., 2012). PCR uses Principal Component Analysis (PCA) (Massy, 1965) of a set of predictive variables before beginning a multiple-linear regression analysis. The objective of PCA in this study is to separate relationships among variables into statistically independent components; it is a matrix factorization modeling technique that transforms a set of observations into uncorrelated latent variables (principal components), which are perpendicular to each other in some alternative vector spaces (Jolliffe, 1986).

PCA is first performed on monthly time series for the 16 meteorological variables (see Table 1) to establish a set of 16 uncorrelated principal components. We then select the first 11 of the principal components that explain more than 99.5% of the variation in pollutants' concentration levels. The data are further aggregated by season [March-April-May (MAM), June-July-August (JJA), September-October-November (SON) and December-January-February (DJF)] before establishing four different transformation models, each valid for the months within that season:

$$PC_j = \sum_{i=1}^{16} e_{i,j} X_i \tag{1}$$

where $e_{i,j}$ indicates the eigenvector between predictor meteorological variables, j and principal components, i. PC refers to a principal component, while X refers to a meteorological variable.

Each principal component has an associated weighting factor, which can then be used to derive the component loading (L) from the following equation:

$$L_{i,j} = \frac{e_{i,j}\sqrt{\lambda_i}}{S_j} \tag{2}$$

where λ_i indicates the eigenvalue of principal components, i, and S_j indicates the variance of meteorological variables, j.

We then compute a regression between the standardized pollutant concentration and the 11 selected principal components as covariates. The pollutant concentration data are standardized in order to reduce the influences from local emissions such as road traffic and thus to remove the local-contributed fluctuation (Karner et al., 2010). We use generalized linear models (GLMs) (Nelder and Wedderburn, 1972), a large category of statistical models for relating responses to linear combinations of predictor variables, to produce a vector of estimated regression coefficients. Compared with the classical normal linear models which assume the distribution of variables are fixed to be normal, and that the identity relationship between linear model and response variable is normal, GLMs loosen some of these restrictive assumptions by involving a flexible link function which allows the response variable to have various relationships with the independent variables, and provide means to analyse non-normal data. GLM has previously been used in many meteorological and air quality studies (e.g. Camalier et al., 2007; Li et al., 2015; Veselý et al., 2009; Zhao et al., 2013).

The vector of estimated regression coefficients is then transformed

back to the scale of the actual covariates, using the selected PCA loadings to derive the final PCR estimator for approximating the regression coefficients which characterizes the original model. The new vector has a dimension of 16 × 1. The transformation is done by the following equation,

$$S_k = L \times B_k \tag{3}$$

where S_k is the 16 × 1 regression coefficient vector of the meteorological variable on the pollutant, k. L is a 16 × 11 matrix of PCA component loading value. B_k is the 11 × 1 vector of the GLM coefficient of the principal components on the pollutant k concentration.

These regression coefficients reflect the sensitivity of air quality on each meteorological variable through model coefficients. Moreover, their contribution to the air quality is defined by changes in meteorological variables and the power of the coefficients of meteorological variables.

3. Results and discussion

3.1. Model evaluation

3.1.1. Evaluation of WRF outputs

The details and evaluations of the WRF dynamic downscaling data are provided by Lin et al. (2015). Herein, we conduct a further evaluation for the WRF outputs used in this study, including surface temperature, pressure and humidity. The evaluation uses meteorological data (temperature, pressure and humidity at surface) at five stations obtained from the Hong Kong Observatory in the period of 1994–2003. The stations include Hong Kong Observatory Headquarter (HKO), Lau Fau Shan (LFS), Shatin (SHA), Ta Kwu Ling (TKL) and Cheung Chau (CC). The stations are selected due to their representative characteristics of regional meteorology (Fig. 1). The refined index of agreement (d_r) (Willmott et al., 2012) in surface temperature, pressure and mixing ratio are estimated to be 0.88, 0.95 and 0.87, respectively, indicating that there are good agreements between the WRF outputs and observation data. The meteorological variables on or above 925 mb are correlated with the radiosonde data recorded in Kings Park (KP), Hong Kong for validation. WRF shows even a stronger correlation (with respect to d_r) with these radiosonde data at three altitudes (925 mb, 850 mb, 700 mb pressure levels), which are respectively 0.96, 0.96, 0.95 for temperature, 0.61, 0.57, 0.44 for dew point and 0.63, 0.72, 0.78 for wind direction.

3.1.2. Evaluation of GLM models

We adopt leave-one-out cross validation to evaluate the accuracy of the GLMs. The predicted results are then compared with the withheld samples. All the samples are withheld in turn, and the process is iterated until all samples are excluded once. Validations are processed for the three monitoring stations.

Fig. 2 compares GLM-predicted and observed air pollutant concentrations averaged by the three monitoring stations. Overall, the predictions and observations show a good agreement ($d_r > 0.7$; $R^2 > 0.572$; $p < 0.001$); the statistical models perform better for O_3 and RSP than for SO_2.

In order to validate the model for the present years, we also apply it to observed meteorological data from 2015 to 2016 provided by both ground station data and radiosonde data obtained from the Hong Kong Observatory. The model estimation of the three pollutants is then compared with observed pollutant data provided by Hong Kong Environment Protection Department. Generally, these comparisons show a good agreement between model projection and observed pollution concentration data: the indices of agreement of O_3, RSP and SO_2 are 0.64, 0.63 and 0.48, respectively.

3.1.3. Performance of GLMs in PRD region

The predictability of the GLMs at locations outside the model calibration region is investigated. The prediction models are applied to Macau and Foshan to predict monthly standardized air pollutant concentration using large scale WRF meteorological data. To estimate the spatial uncertainty in terms of the variation of the coefficients generated from different calibration sites, we use Monte Carlo Analysis based on these coefficients to compute distributions of predicted air pollutant concentrations. Monte Carlo Analysis runs various trials to determine all feasible outcomes and the probability that these outcomes will take place. The distribution of all possible outcomes for each month is compared with the observational data between 2001 and 2003 (Lin et al., 2011) in Fig. 3. By comparing the mean of the model prediction data and the observation data, the refined indices of agreement for RSP are 0.87 and 0.94 in Foshan and Macau, respectively, while the IOAs for SO_2 are 0.67 and 0.66 in Foshan and Macau, respectively. The IOA for O_3 in Macau is 0.43, which is relatively lower than other two species. It is because O_3, as a secondary pollutant, is affected by not only meteorology but other factors such as atmospheric chemistry and its precursors. It is thus expected that contribution of meteorology on O_3 may not be as significant as that on other two pollutants. We note that the observed O_3 in Foshan is not available for this evaluation. Overall, the results show that the GLMs are capable of broadly predicting air pollution within the Pearl River Delta region.

3.2. Sensitivity of air pollutant concentrations to meteorological variables

Using the result of the PCR method, the coefficients of the regression models are analysed to characterize the quantitative relationship between meteorological variables and air pollutant concentration. Regression models are built by each season and each pollutant regarding their unique characteristics. Fig. 4 shows the distribution of the

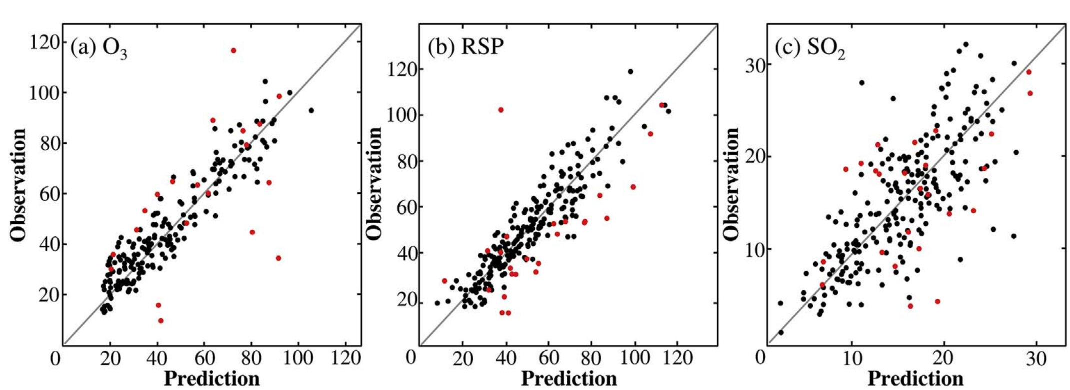

Fig. 2. Scatter plots between prediction (μg/m³) and observation (μg/m³) of monthly means of air pollutants (a: O_3; b: RSP and c: SO_2) with leave-one-out cross validation are displayed in black dots. Those for present year validation are displayed in red. (For interpretation of the references to colour in this figure legend, the reader is referred to the Web version of this article.)

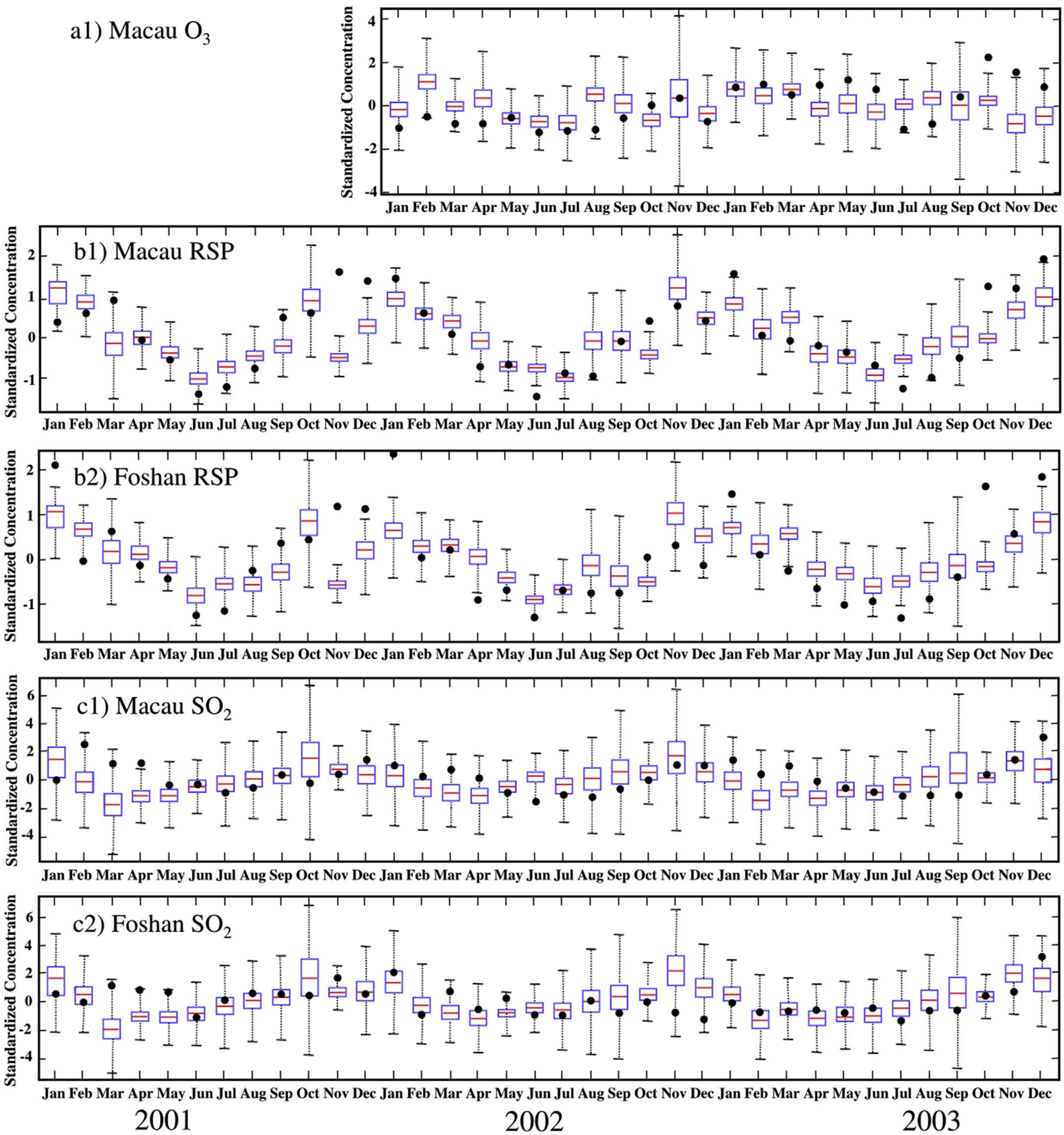

Fig. 3. Comparison between the distributions of model prediction data and the observed data of three air pollutants (a: O_3; b1 & b2: RSP; and c1 & c2: SO_2) in Macau and Foshan, for the sample years of 2001–2003. Prediction data have considered model uncertainty: red line indicates the expected value, blue box indicates the inter-quantile range, and the black bars indicate the 5–95% range. Observed data of RSP and SO_2 are based on Lin et al. (2011); and those of O_3 are based on Região Administrative Especial de Macau (2002, 2003). Note that the O_3 data at Foshan are not available, while O_3 data at Macau are available between 2002 and 2003. (For interpretation of the references to colour in this figure legend, the reader is referred to the Web version of this article.)

standardized coefficients after a series of PCR analyses. Because the meteorological variables are standardized, their corresponding coefficients represent not only their contribution to the projected air pollutant concentration, but also the sensitivity of air quality to the respective variables.

Our results show that the sensitivity values are statistically significant for all studied altitudes. In many occasions, the meteorological variables at higher altitudes yield a larger contribution to the surface pollutant concentration level compared with their corresponding surface values. Moreover, the meteorological variables at higher altitudes have a smaller variance since they are less affected by local scale topographic effects. These results indicate an important role for upper-level meteorological data in influencing surface air quality and a potential mechanism for a meteorological influence on surface pollutant concentrations.

We discuss the sensitivity of different coefficients on the pollutant

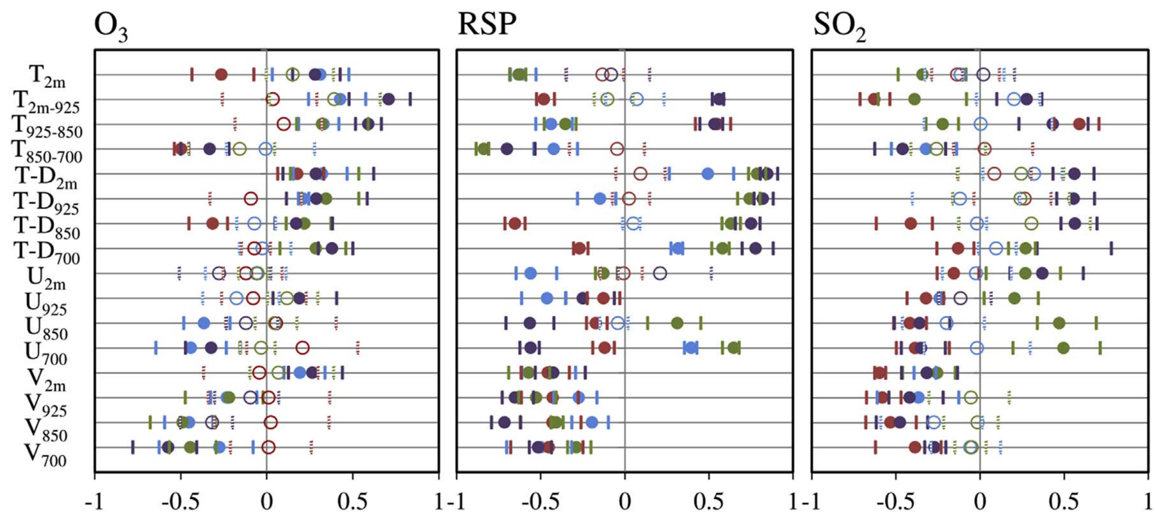

Fig. 4. Transformed Regression Coefficient between the standardized values of the three pollutants and the meteorological variables. Values in circle indicate the model mean, while the small bars indicate the range of model uncertainty between the lowest and highest values. MAM (blue) refers to March-April-May; JJA (red) refers to June-July-August; SON (green) refers to September-October-November; and DJF (purple) refers to December-January-February. Filled circles indicate that the correlation is statistically significant ($p < 0.05$), while empty semi-transparent circles refer to statistically insignificant ($p > 0.05$). (For interpretation of the references to colour in this figure legend, the reader is referred to the Web version of this article.)

concentration with respect to various meteorological variables. In the following discussion, significant air quality–meteorology relationships, which are summarized in Fig. 5, are discussed in the vertical order of meteorological variables shown in the figure.

3.2.1. Surface temperature

Surface temperature (T_{2m}) is significantly negatively correlated with RSP concentration in MAM and SON ($R < -0.582$; $p < 0.011$); the atmosphere is relatively stable when surface temperature is low due to weaker buoyancy force available to drive vertical mixing. Also, lower surface temperature is common during winter monsoon, when large-scale synoptic patterns enhance pollutant concentrations emitted from non-local inland source regions. Such correlation is however not statistically significant in DJF. It is because horizontal wind speed is typically stronger in winter monsoon season than other seasons. Even though low surface temperature may be favorable to stable atmosphere, its associated strong monsoon wind may offset the effect of high atmospheric stability on air pollution accumulation.

O_3 as a secondary pollutant shows a relatively positive correlation with surface temperature in DJF and MAM ($R > 0.487$; $p < 0.016$), possibly due to the important role of temperature during O_3 formation (Jacob and Winner, 2009; Rasmussen et al., 2012). Favorable weather conditions, including cloudless sky and stable atmospheric conditions, help trap O_3 and its precursors within the region during these seasons (Chan and Kwok, 2001; Lam et al., 2005). Yet, a slightly negative correlation between T_{2m} and O_3 concentration is found in JJA ($R < -0.435$, $p < 0.071$), possibly due to the fact that higher temperature leads to unstable atmospheric conditions, uplifting surface air with water vapour for cloud formation.

3.2.2. Vertical temperature gradient

Both positive and negative correlations are revealed between vertical temperature gradient and pollutant concentration at different altitudes. $T_{2m\text{-}925}$ is weakly negatively correlated with RSP ($R < -0.415$; $p < 0.087$) but strongly negatively correlated with SO_2 ($R < -0.708$; $p < 0.001$) in JJA. A small or even negative temperature gradient could hinder vertical air mixing, trapping air pollutants close to the ground. A negative correlation is also found at higher altitudes; $T_{850\text{–}700}$ correlates negatively ($R < -0.500$; $p < 0.048$) with all pollutant concentrations in DJF. One possible explanation for this correlation is that when cold front passes through the region in the winter, denser cold air lifts less dense warm air up, building a layer between two air masses in the mid-troposphere, causing the temperature gradient in the lower troposphere is weaker. The weaker temperature gradient inhibits the removal of surface air pollutants underneath the layer. This idea is further corroborated by the positive correlation between $T_{850\text{–}700}$ and T_{2m} ($R > 0.576$; $p < 0.040$), suggesting that weaker temperature gradients are found under relatively cold conditions.

$T_{2m\text{-}925}$ and $T_{925\text{-}850}$ in DJF exhibit a positive correlation with O_3 and RSP ($R > 0.521$; $p < 0.039$) concentration. Note that small $T_{2m\text{-}925}$ and $T_{925\text{-}850}$ are associated with large V_{700} (stronger southerly wind or weaker northerly wind). This indicates that strong southerlies aloft bring with cleaner and warmer air, contributing to both weaker vertical temperature gradients and less transported pollutants. However, a weak temperature gradient can also imply cloudy and rainy conditions, which both inhibit solar radiation from reaching the surface, and also enhances wet deposition which reduces pollutant concentration levels. SO_2 concentration does not respond the same as O_3 and RSP, as SO_2 concentration does not show the consistent relationship as other two species do. It is because a large proportion of SO_2 emissions along the southern coast of Hong Kong is from marine sources (Lu et al., 2013; Yim et al., 2010) such that the transport mechanism of SO_2 is different from that of other two species.

3.2.3. Wind

To analyse the correlations between wind and pollutant concentration, wind is split into two components: U and V. Regarding the sensitivity of air pollution to regional wind patterns, U component (U_{2m}, U_{925}, U_{850}, U_{700}) does not show a consistent distribution of the coefficients magnitudes: the sign and magnitude of the component change among different seasons and altitudes. The V component (V_{2m}, V_{925}, V_{850}, V_{700}) shows a consistent negative correlation with all the three pollutants, for all the studied altitudes. These relationships are explored using scatter wind roses (see Figs. S2a–c in Supporting Information: SI) which depict the relationship between wind vector components and air quality for all selected altitudes and pollutant species. Months with high pollutant concentration are generally associated with either calm wind or north-easterly wind, particularly from the surface up to 850 mb pressure level. Fig. 4 shows the negative correlation between the V components and pollutant concentration. We note that a reduction in V component implies stronger southerly wind

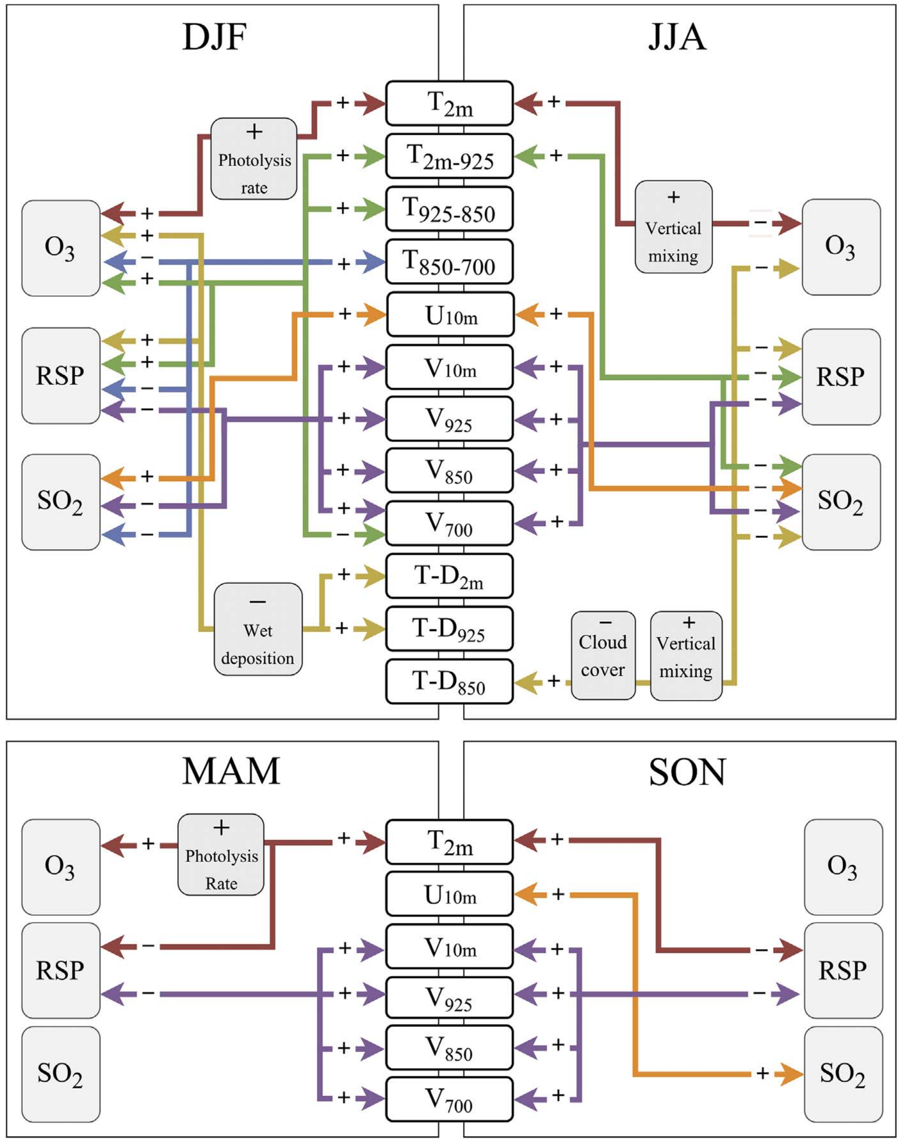

Fig. 5. Significant air quality–meteorology relationships in the study, in various seasons. MAM refers to March-April-May; JJA refers to June-July-August; SON refers to September-October-November; and DJF refers to December-January-February. Positive and negative signs respectively indicate positive and negative correlations between meteorological variables and the corresponding air pollutant.

or weaker northerly wind. The negative correlation between V component and pollutant concentration indicates a higher pollutant level under strong northerlies or weak southerlies conditions. This result is consistent with previous PRD studies that pollutant level increases due to transport of urban plumes by northerly winds (Chan and Kwok, 2001; Lam et al., 2005; Wang et al., 2003).

In the coefficient matrix of SO_2, positive coefficients with U_{10m} are found in SON and DJF (Fig. 4), which are easterly wind (Negative U_{10m}) dominant. Higher SO_2 level is thus associated with weaker easterly wind (Greater U_{10m} value). Negative coefficient with U_{10m} is found in JJA, which is westerly wind (Positive U_{10m}) dominant. Higher SO_2 level is thus associated with weaker westerly wind (Smaller U_{10m} value). Negative correlation is also found between SO_2 concentration and lower altitude V components (V_{925} and V_{850}) in DJF ($R < -0.267$, $p < 0.051$) and JJA ($R < -0.539$, $p < 0.021$). In DJF, strong northerly wind (negative V component) may enhance *trans*-boundary SO_2 to Hong Kong. In JJA, the prevailing wind is due south. Weaker V component along with significant shipping SO_2 emissions at south cause accumulation of SO_2. See Fig. S2c.

The results of both U and V wind components show as expected that calm wind is typically associated with higher pollutant concentration. Similar to previous studies, air pollution is also associated with northeasterly wind that is favorable to regional transport of air pollutants. Our results further reveal that wind components at different altitudes may play various roles on determining pollutant concentration. V_{700} negatively correlates with both O_3 and RSP in DJF, which indicates that northerly wind in the mid troposphere serves as a key factor to transport regional pollutants to the PRD region during winter. Furthermore, wind at ~700 mb pressure height may alter air temperature aloft and thus reduce vertical temperature gradient (increasing atmospheric stability), causing pollutant accumulation (Camps et al., 1997).

3.2.4. *Relative humidity*

Regarding the correlation between relative humidity (T-D) and pollutant concentration, $T\text{-}D_{2m}$ and $T\text{-}D_{925}$ are generally positively correlated with the pollutant concentrations [O_3: $R > 0.577$ ($p < 0.019$); RSP: $R > 0.758$ ($p < 0.001$); SO_2: $R > 0.435$ ($p < 0.092$)] in DJF. Note that a smaller T-D implies relatively higher relative humidity, which can indicate clean marine air (Tai et al., 2010), and is also associated a higher likelihood of precipitation and

thus wet deposition, which has previously been noted by various studies of the same region (Chan and Kwok, 2001; Zhao et al., 2016). Both of these factors can suppress pollutant concentration. Nevertheless, these relationships at higher altitudes in summer are found to be different: pollutant concentration negatively correlates with T-D_{850} in JJA [O_3: $R < -0.459$ ($p < 0.055$); RSP: $R < -0.662$ ($p < 0.003$); SO_2: $R < -0.340$ ($p < 0.168$)]. A possible cause for this is the role of cumulus clouds, which increase atmospheric stability by reducing the low-level lapse rate. Cumulus clouds start to form above 850 mb, which is equivalent to approximately 1500 m above ground. These cumulus clouds often form during summer, hindering direct surface insolation and thus minimising vertical mixing by reducing buoyancy forces (Wood and Bretherton, 2006). This explains the positive correlation of $T_{2m\text{-}925}$ with T-D_{850} ($R > 0.626$ $p < 0.001$) in JJA, which contrasts the less-significant correlation in winter seasons when cumulus clouds are rarer.

3.3. Model application to anomaly studies

This part focuses on understanding the influences of meteorological variables to anomalous air pollutant episodes, which is defined by pollutant concentration outside the central 90% intervals. In the sample observation years of 1994–2003, the central 90% interval concentrations of O_3, RSP and SO_2 are ranged from 29.02 to 61.66 μg/m^3, from 22.63 to 75.77 μg/m^3 and from 9.61 to 21.70 μg/m^3, respectively. We assess the meteorological conditions associated with anomalous pollutant concentrations outside these ranges to better understand the major contributing factors to air pollution episodes in the PRD region. The contribution of a meteorological variable in these air pollution episodes is hereby represented in a percentage of total contribution of all meteorological variables in the air pollution episodes.

For O_3, we note that the most extreme episodes are recorded to occur in SON. Strongly negative V wind components (V_{2m}, V_{925}, V_{850}, V_{700}), which imply strong northerlies, critically influence O_3 anomalies in this season, and contribute altogether 39.53% (34.87%–47.74%) of the total variance averaged over these episodes. Particularly, V_{700} contributes the greatest to the extreme O_3 episodes at four altitudes, with a percentage contribution of 20.81% (16.61%–26.77%) out of total positive contribution by all meteorological variables. This highlights the critical contribution of northerly wind in the mid troposphere to transport regional pollutants to the region, and create extreme surface O_3 episodes.

Extremely high RSP episodes are generally associated with low humidity. These humidity variables (T-D_{2m}, T-D_{925}, T-D_{850}, T-D_{700}) altogether contribute 43.72% (38.38%–47.96%) of the total increase, averaged over all anomaly episodes. As discussed in section 3.2.4, these dry episodes are often associated with inland air and a lack of precipitation and thus wet deposition. These anomalies are also found to appear with weak vertical temperature gradient in the mid troposphere, as illustrated by the fact that small $T_{850\text{-}700}$ makes a positive contribution of 12.87% (12.36%–13.56%) to the total increase to the anomaly episodes.

Our results show that low relative humidity at all four altitudes is found during periods with elevated SO_2, which is consistent to the condition of RSP. These variables altogether contribute to a SO_2 percentage increase of 43.59% (34.86%–48.08%), averaged by all anomalous episodes above 95th percentile.

Overall, strength of northerly wind at all studied altitudes contributes the most to O_3 anomalies which are mostly associated with northerly wind recorded in SON, whereas high RSP and SO_2 anomalies are associated with low relative humidity conditions at all studied altitudes in DJF. Small vertical temperature gradient ($T_{850\text{-}700}$) in mid-troposphere also significantly contributes to the RSP anomalies.

4. Conclusions

This study develops regression models based on both surface and vertical meteorological variables, and comprehensively describe influences of surface and upper level meteorology on various pollutants in different seasons and the contributions of each meteorological variable to anomalous air pollution episodes. We find that the meteorological variables chosen to represent atmospheric stability provide accurate estimates of the air quality metrics, with an Index of Agreement (IOA) of 0.53–0.81. Mid-level troposphere conditions play an important role in impacting surface pollutant levels, comparable to the effect of the surface meteorology.

Our results show that the magnitude and sign of the correlation between air quality and meteorological variables vary in different conditions. Correlations with surface temperature vary for different pollutant species: low surface temperature is associated with north-easterly wind carrying regional pollutants, and less buoyancy force to drive vertical mixing. O_3 differs from the other two pollutants (RSP and SO_2) and its formation is enhanced under higher temperature, which is associated with conditions favorable for photochemistry. Surface humidity negatively correlates with pollutant concentration in most conditions. This could be attributed to moist, clean maritime air and wet deposition in the winter, but this contrasts with positive correlation found during summer which is associated with cumulus clouds. The correlation between air pollutant concentration and wind components reveal the role of north-easterly wind, which provides transport of non-local pollutants from other regions. In other conditions, calm wind favors pollutant accumulation within the PRD region. Temperature gradient shows a variable correlation with air quality for different seasons and for different pollutants, highlighting its role in a variety of pathways including adiabatic effects and synoptic patterns such as cold fronts. Inversion strength could be a driving factor for air pollution problems but the height of inversion layer varies among seasons.

To conclude, our results highlight that meteorological variables at higher altitudes have significant and unique associations with air quality. Such different relationships pinpoint the importance of involving both surface and upper level meteorological variables in statistical models to assess surface air quality. Since air quality is also dependent on emissions, future research should include emissions in the model development to further improve the model performance. In addition, more observation data in the inland areas, once available, should be utilized to further evaluate the model. Moreover, future research may apply the developed statistical models to comprehensively assess the impact of changes in atmospheric condition on regional air quality under the rapid changing climate.

Acknowledgment

This work is jointly funded by the Improvement on Competitiveness in Hiring New Faculties Fund (2013/14) of The Chinese University of Hong Kong; The Vice-Chancellor's Discretionary Fund of The Chinese University of Hong Kong (grant no. 4930744) and the Early Career Scheme of Research Grants Council of Hong Kong (grant no. ECS-24301415). We would like to thank the Hong Kong Environmental Protection Department and the Hong Kong Observatory for providing air quality and meteorological data, respectively. We also would like to thank the technical support from the Information Technology Services Centre (ITSC) at CUHK.

Appendix A. Supplementary data

Supplementary data related to this article can be found at http://dx.doi.org/10.1016/j.atmosenv.2018.02.039.

References

Abdul-Wahab, S.A., Bakheit, C.S., Al-Alawi, S.M., 2005. Principal component and multiple regression analysis in modelling of ground-level ozone and factors affecting its concentrations. Environ. Model. Software 20, 1263–1271.

Baklanov, A., Rasmussen, A., Fay, B., Berge, E., Finardi, S., 2002. Potential and shortcomings of numerical weather prediction models in providing meteorological data for urban air pollution forecasting. Water Air Soil Pollut. Focus 2, 43–60.

Bhattacharjee, P.S., Prasad, A.K., Kamados, M., Singh, R.P., 2007. Influence of a dust storm on carbon monoxide and water vapor over the Indo-Gangetic Plains. J. Geophys. Res.: Atmosphere 112, D18203.

Borger, R., Alexandrov, V., Del Vas, J.J., Lumbreras, J., Rodríguez, E., 2008. A comprehensive sensitivity analysis of the WRF model for air quality applications over the Iberian Peninsula. Atmos. Environ. 42, 8560–8574.

Camalier, L., Cox, W., Dolwick, P., 2007. The effects of meteorology on ozone in urban areas and their use in assessing ozone trends. Atmos. Environ. 41, 7127–7137.

Camps, J., Massons, J., Soler, M.R., Nickerson, E.C., 1997. Pollutant transport in coastal areas with and without background wind. Ann. Geophys. 15, 476–486.

Chan, L.Y., Kwok, W.S., 2001. Roadside suspended particulates at heavily trafficked urban sites of Hong Kong - seasonal variation and dependence on meteorological conditions. Atmos. Environ. 35, 3177–3182.

Che, W., Zheng, J., Wang, S., Zhong, L., Lau, A., 2011. Assessment of motor vehicle emission control policies using Model-3/CMAQ model for the Pearl River Delta region, China. Atmos. Environ. 45, 1740–1751.

Cheng, S., Lam, K.C., 1998. An analysis of winds affecting air pollution concentrations in Hong Kong. Atmos. Environ. 32, 2559–2567.

Cuchiara, G.C., Li, X., Carvalho, J., Rappenglück, B., 2014. Intercomparison of planetary boundary layer parameterization and its impacts on surface ozone concentration in the WRF/Chem model for a case study in Houston/Texas. Atmos. Environ. 96, 175–185.

Filleul, L., Cassadou, S., Médina, S., Fabres, P., Lefranc, A., Eilstein, D., Le Tertre, A., Pascal, L., Chardon, B., Blanchard, M., Declercq, C., 2006. The relation between temperature, ozone, and mortality in nine French cities during the heat wave of 2003. Environ. Health Perspect. 114, 1344.

Fiore, A.M., Dentener, F.J., Wild, O., Cuvelier, C., Schultz, M.G., Hess, P., Textor, C., Schulz, M., Doherty, R.M., Horowitz, L.W., MacKenzie, I.A., 2009. Multimodel estimates of intercontinental source-receptor relationships for ozone pollution. J. Geophys. Res. Atmosphere 114, D04301.

Fiore, A.M., Naik, V., Spracklen, D.V., Steiner, A., Unger, N., Prather, M., Bergmann, D., Cameron-Smith, P.J., Cionni, I., Collins, W.J., Dalsøren, S., 2012. Global air quality and climate. Chem. Soc. Rev. 41, 6663–6683.

Fischer, P.H., Brunekreef, B., Lebret, E., 2004. Air pollution related deaths during the 2003 heat wave in The Netherlands. Atmos. Environ. 38, 1083–1085.

George, J.J., 1960. Weather and Forecasting for Aeronautics. Academic Press 673 pp.

Gu, Y., Yim, S.H.L., 2016. The air quality and health impacts of domestic trans-boundary pollution in various regions of China. Environ. Int. 97, 117–124.

Hassanzadeh, S., Hosseinibalam, F., Omidvari, M., 2008. Statistical methods and regression analysis of stratospheric ozone and meteorological variables in Isfahan. Phys. Stat. Mech. Appl. 387, 2317–2327.

Huang, J.P., Fung, J.C., Lau, A.K., Qin, Y., 2005. Numerical simulation and process analysis of typhoon-related ozone episodes in Hong Kong. J. Geophys. Res. Atmosphere 110, D05301.

IPCC. Climate Change, 2014. In: Pachauri, R.K., Meyer, L.A. (Eds.), Synthesis Report. Contribution of Working Groups I, II and III to the Fifth Assessment Report of the Intergovernmental Panel on Climate Change, pp. 1–151 Geneva, Switzerland, 2014.

Jacob, D.J., Winner, D.A., 2009. Effect of climate change on air quality. Atmos. Environ. 43, 51–63.

Jeričević, A., Grisogono, B., 2006. The critical bulk Richardson number in urban areas: verification and application in a numerical weather prediction model. Tellus A 58, 19–27.

Jolliffe, I.T., 1986. Principal Component Analysis and Factor Analysis, in: Principal component analysis. Springer New York, pp. 115–128.

Kalnay, E., Kanamitsu, M., Kistler, R., Collins, W., Deaven, D., Gandin, L., Iredell, M., Saha, S., White, G., Woollen, J., Zhu, Y., 1996. The NCEP/NCAR 40-year reanalysis project. Bull. Am. Meteorol. Soc. 77, 437–471.

Karner, A.A., Eisinger, D.S., Niemeier, D.A., 2010. Near-roadway air quality: synthesizing the findings from real-world data. Environ. Sci. Technol. 44, 5334–5344.

Kistler, R., Collins, W., Saha, S., White, G., Woollen, J., Kalnay, E., Chelliah, M., Ebisuzaki, W., Kanamitsu, M., Kousky, V., van den Dool, H., 2001. The NCEP–NCAR 50–year reanalysis: monthly means CD–ROM and documentation. Bull. Am. Meteorol. Soc. 82, 247–267.

Kutner, M.H., Nachtsheim, C., Neter, J., 2004. Applied Linear Regression Models. McGraw-Hill/Irwin.

Lam, K.S., Wang, T.J., Wu, C.L., Li, Y.S., 2005. Study on an ozone episode in hot season in Hong Kong and transboundary air pollution over Pearl River Delta region of China. Atmos. Environ. 39, 1967–1977.

Lee, Y.C., Savtchenko, A., 2006. Relationship between air pollution in Hong Kong and in the Pearl River delta region of south China in 2003 and 2004: an analysis. J Appl. Meteorol. Clim. 45, 269–282.

Li, L., Qian, J., Ou, C.Q., Zhou, Y.X., Guo, C., Guo, Y., 2014. Spatial and temporal analysis of Air Pollution Index and its timescale-dependent relationship with meteorological factors in Guangzhou, China, 2001–2011. Environ. Pollut. 190, 75–81.

Li, T., Yan, M., Ma, W., Ban, J., Liu, T., Lin, H., Liu, Z., 2015. Short-term effects of multiple ozone metrics on daily mortality in a megacity of China. Environ. Sci. Pollut. Res. Int. 22, 8738–8746.

Lin, C.Y., Chua, Y.J., Sheng, Y.F., Hsu, H.H., Cheng, C.T., Lin, Y.Y., 2015. Altitudinal and latitudinal dependence of future warming in Taiwan simulated by WRF nested with ECHAM5/MPIOM. Int. J. Climatol. 35, 1800–1809.

Lin, M., Chan, I.N., Chan, C.Y., Wang, X.M., Dong, H.Y., 2011. Emerging air pollution issues in changing Pearl River delta of south China. In: The Impact of Air Pollution on Health, Economy, Environment and Agricultural Sources, InTech.

Lo, J.C., Lau, A.K., Fung, J.C., Chen, F., 2006. Investigation of enhanced cross-city transport and trapping of air pollutants by coastal and urban land-sea breeze circulations. J. Geophys. Res.: Atmos. 111, D14104.

Lu, Q., Zheng, J., Ye, S., Shen, X., Yuan, Z., Yin, X., 2013. Emission trends and source characteristics of SO_2, NO_X, PM10 and VOCs in the Pearl River Delta region from 2000 to 2009. Atmos. Environ. 76, 11–20.

Luo, M., Hou, X., Gu, Y., Lau, N.C., Yim, S.H.L., 2017. Trans-boundary air pollution in a city under various atmospheric conditions. Sci. Total Environ. 618, 132–141.

Maenhaut, W., Cornille, P., Pacyna, J.M., Vitols, V., 1989. Trace element composition and origin of the atmospheric aerosol in the Norwegian Arctic. Atmos. Environ. (1967) 23, 2551–2569.

Massy, W.F., 1965. Principal components regression in exploratory statistical research. J. Am. Stat. Assoc. 60, 234–256.

Meng, Z.Y., Xu, X.B., Wang, T., Zhang, X.Y., Yu, X.L., Wang, S.F., Lin, W.L., Chen, Y.Z., Jiang, Y.A., An, X.Q., 2010. Ambient sulfur dioxide, nitrogen dioxide, and ammonia at ten background and rural sites in China during 2007–2008. Atmos. Environ. 44, 2625–2631.

Miller, R., 1972. Notes on Analysis and Severe Storm Forecasting Procedures of the Air Force Global Weather Central. Technical Report 200, AWS, U.S. Air Force, 102.

Nelder, J.A., Wedderburn, R.W.M., 1972. Generalized linear models. J. Roy. Stat. Soc. A 135 (3), 370–384.

Peng, G., Wang, X., Wu, Z., Wang, Z., Yang, L., Zhong, L., Chen, D., 2011. Characteristics of particulate matter pollution in the Pearl River Delta region, China: an observational-based analysis of two monitoring sites. J. Environ. Monit. 13, 1927–1934.

Pielke, R.A., Uliasz, M., 1998. Use of meteorological models as input to regional and mesoscale air quality models—limitations and strengths. Atmos. Environ. 32, 1455–1466.

Rajab, J.M., MatJafri, M.Z., Lim, H.S., 2013. Combining multiple regression and principal component analysis for accurate predictions for column ozone in Peninsular Malaysia. Atmos. Environ. 71, 36–43.

Ramsey, N.R., Klein, P.M., Moore, B., 2014. The impact of meteorological parameters on urban air quality. Atmos. Environ. 86, 58–67.

Rasmussen, D.J., Fiore, A.M., Naik, V., Horowitz, L.W., McGinnis, S.J., Schultz, M.G., 2012. Surface ozone-temperature relationships in the eastern US: a monthly climatology for evaluating chemistry-climate models. Atmos. Environ. 47, 142–153.

Região Administrative Especial de Macau, 2002. Relatório anual da qualidade do ar ano de 2002. Centro de clima e ambiente atmosférico, direcção dos serviços de meteorológicos e geofísicos, pp. 1–64. http://www.smg.gov.mo/smg/airQuality/pdf/IQA_2002.pdf.

Região Administrative Especial de Macau, 2003. Relatório anual da qualidade do ar ano de 2003. Centro de clima e ambiente atmosférico, direcção dos serviços de meteorológicos e geofísicos, pp. 1–64. http://www.smg.gov.mo/smg/airQuality/pdf/IQA_2003.pdf.

Samet, J., Zeger, S., Kelsall, J., Xu, J., Kalkstein, L., 1998. Does weather confound or modify the association of particulate air pollution with mortality?: an analysis of the Philadelphia data, 1973–1980. Environ. Res. 77, 9–19.

Shir, C.C., Shieh, L.J., 1974. A generalized urban air pollution model and its application to the study of SO_2 distributions in the St. Louis metropolitan area. J. Appl. Meteorol. 13, 185–204.

Sillman, S., 1999. The relation between ozone, NOx and hydrocarbons in urban and polluted rural environments. Atmos. Environ. 33, 1821–1845.

Sillman, S., Samson, P.J., 1995. Impact of temperature on oxidant photochemistry in urban, polluted rural and remote environments. J. Geophys. Res. Atmosphere 100, 11497–11508.

Skamarock, W.C., Klemp, J.B., 2008. A time-split nonhydrostatic atmospheric model for weather research and forecasting applications. J. Comput. Phys. 227, 3465–3485.

Statheropoulos, M., Vassiliadis, N., Pappa, A., 1998. Principal component and canonical correlation analysis for examining air pollution and meteorological data. Atmos. Environ. 32, 1087–1095.

Tai, A.P., Mickley, L.J., Jacob, D.J., 2010. Correlations between fine particulate matter (PM2.5) and meteorological variables in the United States: implications for the sensitivity of PM2.5 to climate change. Atmos. Environ. 44, 3976–3984.

Tai, A.P., Mickley, L.J., Jacob, D.J., Leibensperger, E.M., Zhang, L., Fisher, J.A., Pye, H.O.T., 2012. Meteorological modes of variability for fine particulate matter (PM2.5) air quality in the United States: implications for PM2.5 sensitivity to climate change. Atmos. Chem. Phys. 12, 3131–3145.

Veselý, V., Tonner, J., Hrdlivčková, Z., Michálek, J., Kolář, M., 2009. Analysis of PM10 air pollution in Brno based on generalized linear model with strongly rank-deficient design matrix. Environmetrics 20, 676–698.

Wang, F., Chen, D.S., Cheng, S.Y., Li, M.J., 2009. Impacts of air pollutant transport based on air trajectory clustering. Res. Environ. Sci. 22, 637–642.

Wang, T., Poon, C.N., Kwok, Y.H., Li, Y.S., 2003. Characterizing the temporal variability and emission patterns of pollution plumes in the Pearl River Delta of China. Atmos. Environ. 37, 3539–3550.

Wang, T., Wu, Y.Y., Cheung, T.F., Lam, K.S., 2001. A study of surface ozone and the relation to complex wind flow in Hong Kong. Atmos. Environ. 35, 3203–3215.

Wang, X.K., Lu, W.Z., 2006. Seasonal variation of air pollution index: Hong Kong case study. Chemosphere 63, 1261–1272.

Wang, X., Liao, J., Zhang, J., Shen, C., Chen, W., Xia, B., Wang, T., 2014. A numeric study of regional climate change induced by urban expansion in the Pearl River delta,

China. J. Appl. Meteorol.Clim. 53, 346–362.
Willmott, C.J., Robeson, S.M., Matsuura, K., 2012. A refined index of model performance. Int. J. Climatol. 32, 2088–2094.
Wong, T.W., San Tam, W.W., Yu, I.T.S., Lau, A.K.H., Pang, S.W., Wong, A.H., 2013. Developing a risk-based air quality health index. Atmos. Environ. 76, 52–58.
Wood, R., Bretherton, C.S., 2006. On the relationship between stratiform low cloud cover and lower-tropospheric stability. J. Clim. 19, 6425–6432.
Wu, D., Tie, X., Li, C., Ying, Z., Lau, A.K.H., Huang, J., Deng, X., Bi, X., 2005. An extremely low visibility event over the Guangzhou region: a case study. Atmos. Environ. 39, 6568–6577.
Yim, S.H.L., Fung, J.C.H., Lau, A.K.H., 2010. Use of high-resolution MM5/CALMET/CALPUFF system: SO2 apportionment to air quality in Hong Kong. Atmos. Environ. 44 (38), 4850–4858.
Zhang, H., Wang, Y., Hu, J., Ying, Q., Hu, X.M., 2015. Relationships between meteorological parameters and criteria air pollutants in three megacities in China. Environ. Res. 140, 242–254.
Zhang, R., Li, Q., Zhang, R., 2014. Meteorological conditions for the persistent severe fog and haze event over eastern China in January 2013. Sci. China Earth Sci. 57, 26–35.
Zhao, C., Liu, X., Qian, Y., Yoon, J., Hou, Z., Lin, G., McFarlane, S., Wang, H., Yang, B., Ma, P.L., Yan, H., 2013. A sensitivity study of radiative fluxes at the top of atmosphere to cloud-microphysics and aerosol parameters in the community atmosphere model CAM5. Atmos. Chem. Phys. 13, 10969.
Zhao, W., Fan, S., Guo, H., Gao, B., Sun, J., Chen, L., 2016. Assessing the impact of local meteorological variables on surface ozone in Hong Kong during 2000–2015 using quantile and multiple line regression models. Atmos. Environ. 144, 182–193.
Zheng, J., Zhang, L., Che, W., Zheng, Z., Yin, S., 2009. A highly resolved temporal and spatial air pollutant emission inventory for the Pearl River Delta region, China and its uncertainty assessment. Atmos. Environ. 43, 5112–5122.
Zoumakis, N.M., Kelessis, A.G., 1991. The dependence of the bulk Richardson number on stability in the surface layer. Boundary-Layer Meteorol. 57, 407–414.